Journal of Power Sources 184 (2008) 462–468

Contents lists available at ScienceDirect

Journal of Power Sources

journal homepage: www.elsevier.com/locate/jpowsour

Li_2MSiO_4 (M = Fe and/or Mn) cathode materials

R. Dominko*

National Institute of Chemistry, Hajdrihova 19, SI-1000 Ljubljana, Slovenia

ARTICLE INFO

Article history:
Received 19 December 2007
Received in revised form 28 February 2008
Accepted 29 February 2008
Available online 18 March 2008

Dedicated to Professor Besenhard.

Keywords:
Li_2FeSiO_4
Li_2MnSiO_4
Orthosilicates
Structure stability
Li-ion batteries

ABSTRACT

Two iso-structural end members of the family of orthosilicates, i.e. Li_2MSiO_4 (M = Mn and Fe) and their solid solutions, were prepared and electrochemically characterized for potential use in Li-ion batteries. Due to the low specific conductivity ($\sim 5 \times 10^{-16}$ S cm^{-1} for Li_2MnSiO_4 and $\sim 6 \times 10^{-14}$ S cm^{-1} for Li_2FeSiO_4 at room temperature), small particles in an intimate contact with a conducting phase (i.e. carbon) are needed. Li_2MSiO_4/C composites (M = Mn and/or Fe) prepared by the Pechini synthesis generally leads to 30–50 nm large particles embedded in a carbon matrix. The amount of carbon in the composite is close to 10 wt.% for the Li_2FeSiO_4/C composite and slightly more than 5 wt.% for the Li_2MnSiO_4/C composite. In situ XRD experiment confirms a structural collapse of Li_2MnSiO_4 and the observed structural stability is completely different for Li_2FeSiO_4, which undergoes a fully reversible two-phase transition. Solid solutions between Li_2MnSiO_4 and Li_2FeSiO_4 in principle lead to higher capacities (>1e$^-$ per transition metal is feasible). For a long-term operation the cut-off voltage should be properly chosen. Electrochemical characterisation and in situ XRD experiments suggest the use of cut-off voltage close to 4.2 V.

1. Introduction

The need for large-scale Li-ion batteries in HEV, emergency power and dispersed electric power concepts is a motivation for continuous research and innovations in this field [1]. Large-scale Li-ion batteries should fulfil a variety of safety, environmental, price and energy density demands. In this context, polyanion-type cathode materials with a cheap and environmentally friendly transition metal element (i.e. Mn and Fe), seems a good choice. Indeed, after the first report from Goodenough and coworkers [2], polyanion-type cathode materials have gained a lot of attention. While the electrochemical performance of $LiFePO_4$ has been widely studied [3–5], only a few reports characterize the structural and electrochemical performance of the iso-structural $LiMnPO_4$ [6,7]. A further step from the olivine-type cathode materials was done by Nyten et al. [8] who synthesized, electrochemically and structurally characterized a Li_2FeSiO_4 cathode material [9,10]. They showed a reversible lithium exchange with exploration of the Fe^{II}/Fe^{III} redox couple within the electrolyte stability window. Their results strongly favour the family of orthosilicates as new and cheap cathode materials for large-scale battery applications which can operate at higher temperatures [11]. We recently showed that both the structure and the electrochemical performance are highly dependant on the synthesis conditions [12]. The exchange of Fe with Mn leads to an iso-structural material, i.e. Li_2MnSiO_4, with a higher working voltage and with a possibility to obtain a cathode material where, at least in theory, a two-electron electrochemical reaction per transition metal (exploitation of the Mn^{II}/Mn^{III} and Mn^{III}/Mn^{IV} redox couples) becomes feasible [13–15].

The structure of Li_2MSiO_4 (M = Fe, Mn or Co) [16] can be associated to lithiophosphate (Li_3PO_4), which is known to crystallize at least in three different polymorphs (a low temperature form – "α-phase" in the $Pmn2_1$ space group; in a high temperature form – "β-phase" in the *Pmnb* space group; and a third polymorph – "γ-phase" which is detected to occur above $T = 1170\,^{\circ}C$ [17]). Due to the very small differences in the formation energies of the three polymorphs, the as-prepared samples usually occur as mixtures of two or even all three polymorphs, with detectable cation disorder which causes considerable difficulties in the structural refinement.

Preliminary measurements have shown that a mixture of the $Pmn2_1$ and *Pmnb* polymorphs of Li_2MnSiO_4 transforms into an amorphous phase during the first lithium extraction and that the crystalline material is not obtained anymore after consequent reduction process. Most likely, this process is responsible for the low reversibility of Li_2MnSiO_4/C samples. A report by Yang and coworkers [18] indicates that a proper mixture of mixed manganese–iron orthosilicates can deliver more that one electron per transition metal in a wide potential range (between 4.8 and 1.5 V vs. lithium reference). The cycling stability of mixed samples is very similar to the one observed for pure Mn-based orthosilicates [14,15]. To get a further insight into the structural changes, we have performed DFT calculations, recently. The calculations clearly predicted a stabilizing effect of iron if a solid solution of man-

* Tel.: +386 14760362; fax: +386 14760422.
E-mail address: Robert.Dominko@ki.si.

0378-7753/$ – see front matter © 2008 Elsevier B.V. All rights reserved.
doi:10.1016/j.jpowsour.2008.02.089

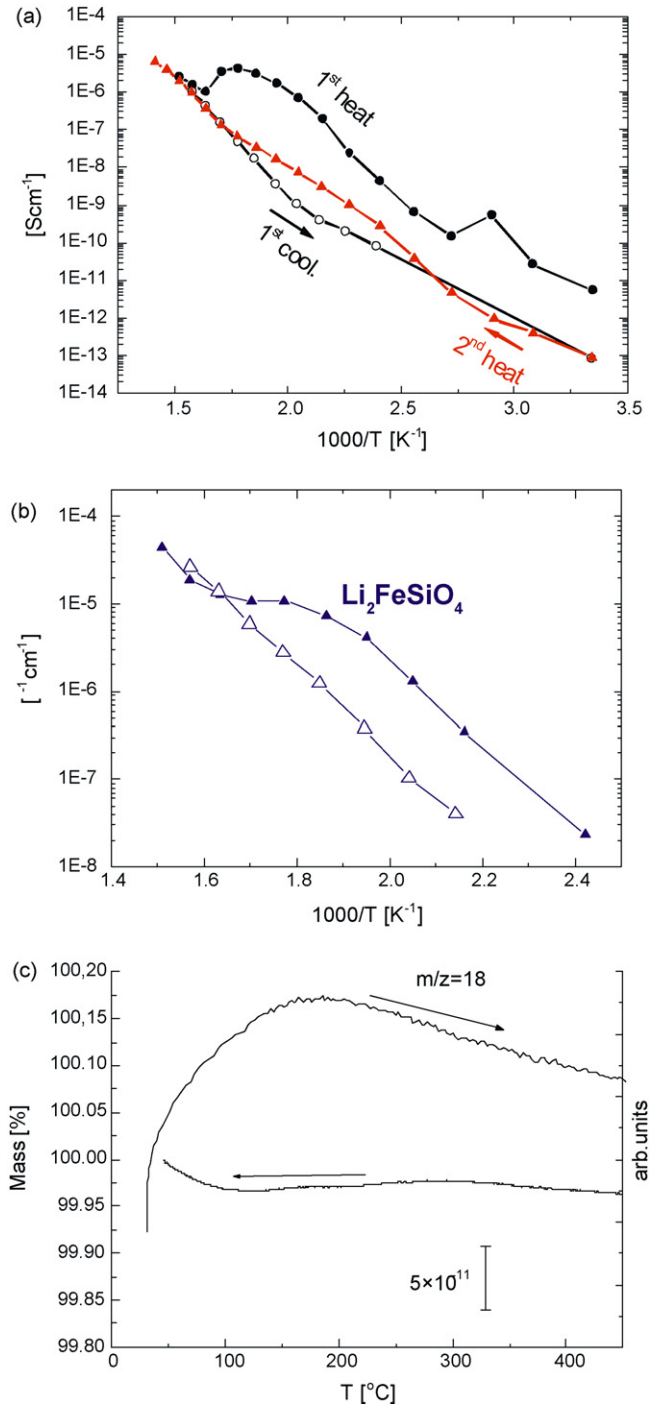

Fig. 1. (a) Temperature dependence of conductivity for Li_2MnSiO_4 during the first heating (filled circles) and first cooling (open circles) of pellet. Filled triangles correspond to the values during the second heating, (b) temperature dependence of conductivity for Li_2FeSiO_4 during the first heating (filled triangles) and the first cooling (open triangles) of pellet and (c) TG–MS of Li_2MnSiO_4, after the sample was exposed to the air atmosphere for a week. The $m/z = 18$ presents desorption of water.

ganese and iron in the lithium orthosilicate structure is formed [15].

The recent synthesis, structural characterization and preliminary electrochemical characterization of Li_2MnSiO_4 [13–15] and as well as of Li_2FeSiO_4 [12,13,15] were a motivation for further systematic studies of the orthosilicate family involving a more detailed electrochemical characterisation combined with in situ XRD characterization. It is the aim of this work to show the electrochemical performance and the structural stability of Li_2FeSiO_4 and Li_2MnSiO_4 and to compare the observed results with the results obtained for mixed manganese–iron lithium orthosilicates.

2. Experimental

Li_2MSiO_4 (M = Mn and/or Fe) were synthesized with three different synthesis methods, i.e. a hydrothermal synthesis [13], a modified Pechini synthesis and a standard Pechini synthesis [19]. The starting precursors for Li_2FeSiO_4 prepared by hydrothermal synthesis were lithium hydroxide (Aldrich), SiO_2–cabosil M5 (Riedel-de Haën) and Fe(II) chloride tetrahydrate (Aldrich) in molar ratio 4:1:1. The slurry was prepared and sealed into a Teflon-lined stainless-steal autoclave under Ar atmosphere and left for 14 days at 150 °C. After the hydrothermal treatment had been completed, the resulting greyish-green powder was rinsed several times with a distilled water and dried under vacuum at 80 °C for 24 h.

Preparation of Li_2FeSiO_4 by the Pechini synthesis was carried out by dispersing Cabosil M5 SiO_2 particles (Riedel-de Haën), Li acetate dihydrate (Aldrich), ethylene glycol (Riedel-de Haën) and citric acid in water in a ratio of 1:2:1:2 for 2 h (with use of ultrasound) prior the addition of Fe(III) citrate (Aldrich). The mixture containing Li, Fe and SiO_2 in a molar ratio of 2:1:1 was stirred for an hour and maintained during the night to enable formation of sol. The sol was dried at 80 °C for at least 24 h. After thorough grinding with a mortar and pestle, the obtained xerogel was heat treated in a gas-tight quartz tube with a constant flow of CO/CO_2 (approximately 100 ml min^{-1}). The initial heating rate was 10 °C min^{-1}. After reaching 700 °C, the samples were maintained at that temperature for 1 h and then left to cool slowly down to room temperature.

Li_2MnSiO_4 was synthesised via the standard Pechini method as well as using a modified Pechini synthesis. For the standard Pechini synthesis the starting precursors were lithium acetate dihydrate (Aldrich), manganese acetate tetrahydrate (Aldrich) and SiO_2 particles cabosil M5 (Riedel-de Haën). Citric acid (Aldrich) and ethylene glycol (Riedel-de Haën) were used as complexation agents for SiO_2 particles in a molar ratio of 1:2:1, with respect to the quantity of added SiO_2. The solution of Li, Mn and SiO_2 in a molar ratio of 2:1:1 was stirred for an hour and maintained during the night before drying at 60 °C for at least 24 h. After thorough grinding with a mortar and pestle, the obtained powder was heat treated in a gas-tight quartz tube with a moderate but constant flow of Ar 5.0 (purity more than 99.999 vol.%). The initial heating rate was 10 °C min^{-1}. After reaching a pre-selected temperature, the samples were maintained at that temperature and then left to cool down to room temperature. The preparation of Li_2MnSiO_4 via the modified Pechini synthesis was carried out according to the same procedure, except that as a Li salt Li-nitrate (Aldrich) was used and the quantity of citric acid and ethylene-glycol was reduced to one quarter with respect to the one described above. The heating procedure was the same as in the case of carbon containing samples except that Ar + 5 wt.% of H_2 was used as atmosphere during the heating procedure.

Mixed manganese—iron sample were prepared using the standard Pechini synthesis, whereby Fe-citrate (Aldrich) and Mn acetate tetrahydrate (Aldrich) were used as Fe and Mn sources, respectively. The sample was heat treated in a CO/CO_2 (1:1) atmosphere at 700 °C for 1 h.

The obtained samples were directly transferred into a glovebox, grinded with 10 wt.% of added acetylene black and loosely pressed onto a circular Al foil with a diameter of 16 mm (2 cm^2). The active material mass was always between 5 and 6 mg. The electrochemical characteristics were measured in vacuum-sealed triplex foil (coffee bag foil) cells. The electrolyte used was a 0.8 M solution

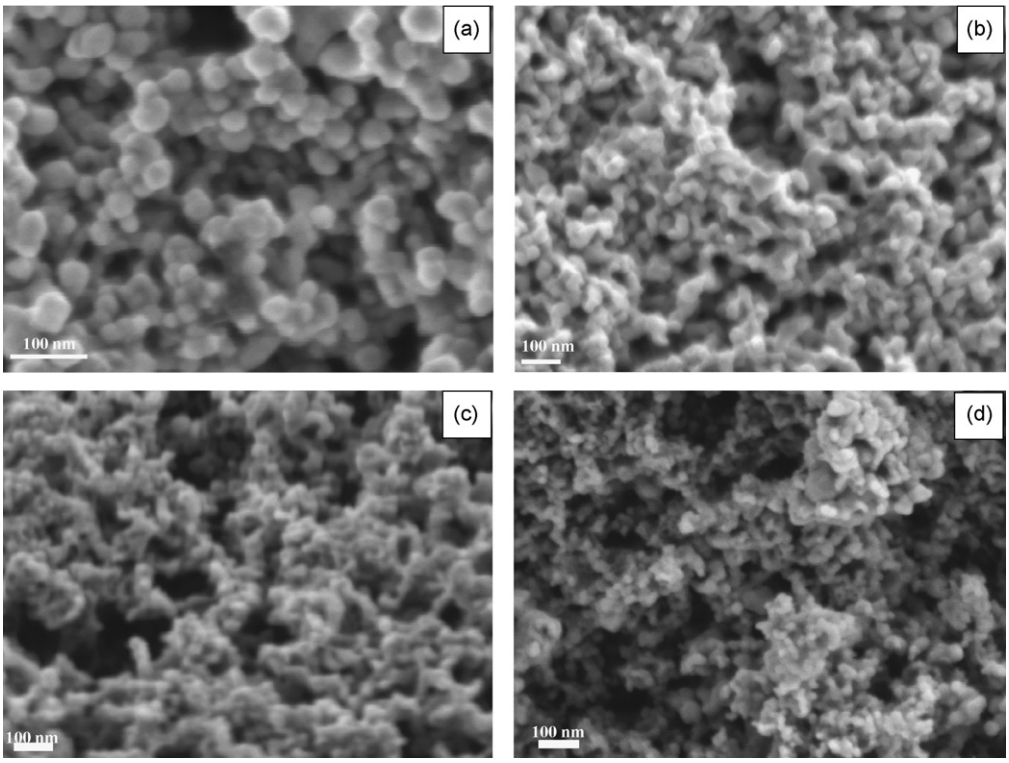

Fig. 2. SEM micrographs of samples obtained by the Pechini method (a) Li_2FeSiO_4/C composite, (b) $Li_2Mn_{0.25}Fe_{0.75}SiO_4$/C composite, (c) $Li_2Mn_{0.5}Fe_{0.5}SiO_4$/C composite and (d) Li_2MnSiO_4/C composite.

of LiBOB (lithium bis(oxalato) borate, Chemetall) in EC:DEC (1:1 ratio by volume) purchased from Aldrich. Solvents and the salt were used as received. The working and the counter electrode consisting of metallic lithium were separated with a glass wool separator. The electrochemical measurements were performed using a VMP3 potentiostat/galvanostat at a constant temperature of 60 °C with a current density corresponding to C/20, if not stated otherwise.

Surfaces of samples were observed and analyzed with a field emission scanning electron microscope (FE-SEM, Supra 35 VP, Carl Zeiss, Germany) using in-lens detector at an accelerating voltage of 1 kV and a working distance of 3–4 mm. In situ X-ray powder diffraction patterns were collected in a home made cell on a Simens D-5000 diffractometer in reflection (Bragg–Brentano) mode using Cu Kα radiation with Autolab cycling/data recording system. Data were collected in the range 22° and 40° in steps of 0.04°. The cycling rate for Li_2FeSiO_4 was C/50 in the potential window from 2.0 to 4.1 V versus metallic lithium reference. Each XRD scan corresponded to a compositional change of $\Delta x = 0.05$. The cycling rate for $Li_2Fe_{0.75}Mn_{0.25}SiO_4$ was C/50 in the potential window from 2.0 to 4.2 V and 4.5 V versus metallic lithium reference. Each XRD scan corresponded to a compositional change of $\Delta x = 0.05$. The cycling rate for Li_2MnSiO_4 was C/50 in the potential window from 2.0 to 4.8 V versus metallic lithium reference. Each XRD scan corresponded to a compositional change of $\Delta x = 0.2$.

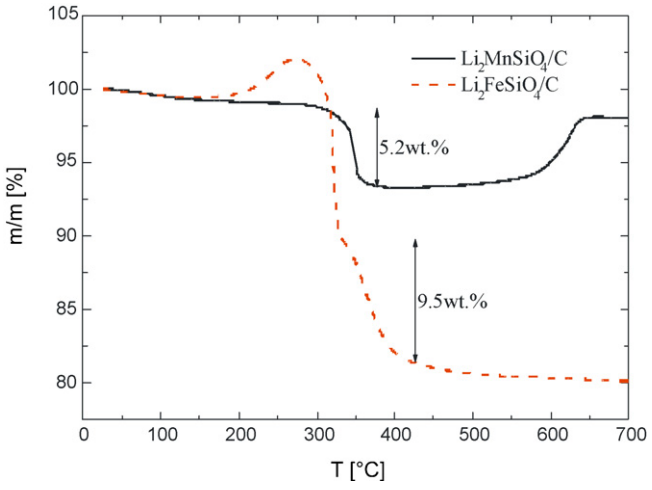

Fig. 3. TG curves for Li_2MnSiO_4/C (solid line) and Li_2FeSiO_4/C (dashed line) composites in air.

The carbon content was calculated from thermogravimetric data obtained using a Mettler Toledo TGA/SDTA 851^e thermoanalyzer. The TG curves were recorded in an oxygen flow of 100 ml min^{-1}. The baseline was subtracted in all cases.

For specific conductivity measurements, samples without carbon (Li_2MnSiO_4 obtained by the modified Pechini synthesis and Li_2FeSiO_4 obtained by the hydrothermal synthesis) were pressed into pellets. The contacts were made by painting both basal planes by a Pt paste. The temperature-dependent impedance spectra were recorded by putting the sample into a gas-tight quartz tube equipped with appropriately shielded Pt wires and thermocouples. Prior to and during the heating, an inert atmosphere was maintained within the tube using Ar 5.0 (purity more than 99.999 vol.%). The impedance spectra were recorded in a frequency range of 1 MHz to 10 mHz with a Solartron 1260 instrument.

3. Results and discussion

Considering the proposed structure [9,13,15] where M (M = Fe or Mn) is tetragonally co-ordinated with oxygen atoms, and MO_4 tetrahedrons are isolated with SiO_4 and LiO_4 tetrahedrons, it is not surprising that the measurements of inherent materials conductivity give values indicating a semiconducting-to-insulating

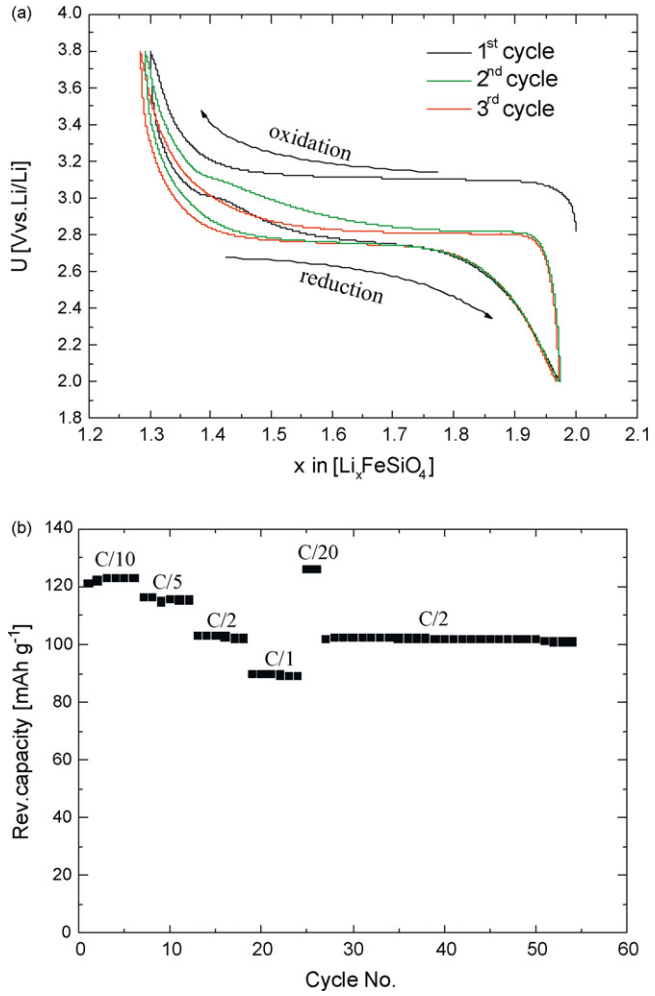

Fig. 4. (a) Discharge–charge curves for first three cycles for Li_2FeSiO_4/C composite at C/20 cycling rate and (b) cycling performance of Li_2FeSiO_4/C composite at different current densities (marked as C-rates).

behaviour of Li_2MSiO_4 (M = Fe or Mn)-based cathode materials. For the specific conductivity measurements, carbon-free Li_2MnSiO_4 sample (prepared by a modified Pechini synthesis method) and Li_2FeSiO_4 sample, synthesised by a hydrothermal method [13] were used. The specific conductivities calculated from the impedance measurements of Li_2MnSiO_4 pellets as a function of temperature are shown in Fig. 1a while the corresponding values for Li_2FeSiO_4 pellet are shown in Fig. 1b (the points are connected with a line for easier eye guidance). The relatively high values of conductivities measured at low temperatures are due to the adsorbed water on the particles surface. The presence of adsorbed water on the surface of the particles was confirmed by TGA–MS (Fig. 1c). The measurement was performed in an argon flow. The detected change of mass for about 0.02 wt.% is accompanied with evolution of water, as determined by mass spectroscopy. According to this result, the main reason for the observed hysteresis between the first heating and cooling is most likely the presence of adsorbed water. Namely, measurements during the second heating are following the first cooling points (Fig. 1a). The specific conductivity for Li_2MnSiO_4 and Li_2FeSiO_4 samples at 60 °C and at room temperature has been determined by extrapolation of the cooling curve to these temperatures. The obtained values at 60 °C are 3×10^{-14} S cm^{-1} for Li_2MnSiO_4 and approximately 2×10^{-12} S cm^{-1} for Li_2FeSiO_4. The specific conductivity at room temperature is by ca. two orders of magnitude lower: 5×10^{-16} S cm^{-1} for Li_2MnSiO_4 and 6×10^{-14} S cm^{-1} for Li_2FeSiO_4. The calculated activation energy for both samples is close to 1 eV [15].

These almost insulating properties of Li_2MnSiO_4 and Li_2FeSiO_4 suggest that, in order to be used in Li-ion batteries, these materials should be prepared in a form of nanoparticulate or nanotextured material that is in intimate contact with an electron-conducting phase (e.g. with a carbon material), as well as with an ion-conducting phase (electrolyte). Li_2MSiO_4 (M = Fe and/or Mn) samples were prepared using the Pechini method that generally leads to particles embedded in a carbon matrix with a particle size from 30 to 50 nm. Typical SEM micrographs of Li_2FeSiO_4/C, $Li_2Fe_{0.75}Mn_{0.25}SiO_4$/C, $Li_2Fe_{0.5}Mn_{0.5}SiO_4$/C and Li_2MnSiO_4/C are shown in Fig. 2a–d. The particles are well separated which allows a good ionic contact. The carbon content in Li_2MSiO_4/C composites is slightly more than 5 wt.% for the Li_2MnSiO_4/C composite and close to 10 wt.% for the Li_2FeSiO_4/C composite (with the assumption that the second mass decrease in TG is due to carbon burn-off) (Fig. 3) [20].

The Li_2FeSiO_4/C sample shown in Fig. 2a exhibits a typical voltage plateau profile decrease (Fig. 4a) during the first three cycles [8,9] and can deliver more than 120 mAh g^{-1} at low-current densities (C/20, C/10) or close to 100 mAh g^{-1} at moderate current densities (C/2) with an excellent cycling stability (Fig. 4b). The capacity was calculated on the basis of as prepared sample, neither the amount of in situ formed carbon nor the impurities were deduced for this calculation.

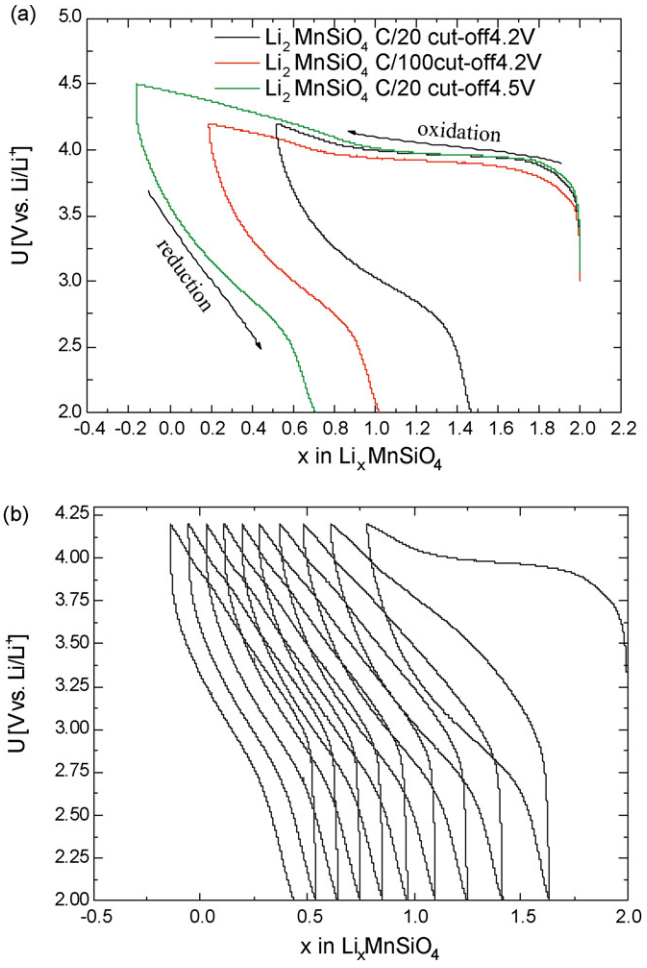

Fig. 5. Cycle performance of Li_2MnSiO_4 materials: (a) differences in the first cycle performance at C/100 and C/20 rates for Li_2MnSiO_4/C composite at cut-off voltage 4.2 and 4.5 V and (b) cycling performance of Li_2MnSiO_4/C composite.

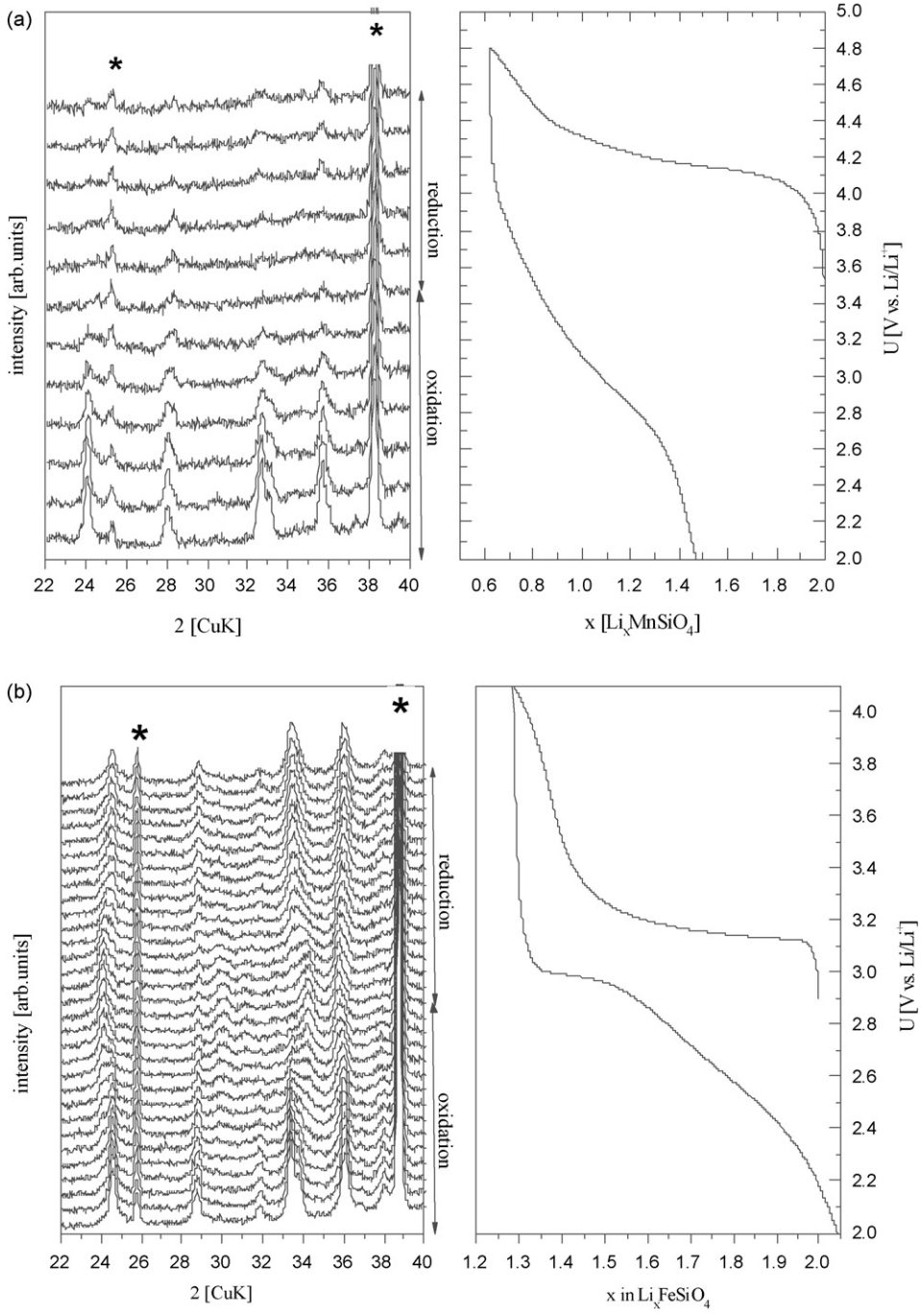

Fig. 6. (a) in situ X-ray diffraction patterns for Li_2FeSiO_4/C done at C/50 rate with $\Delta x = 0.05$ and (b) in situ X-ray diffraction patterns for Li_2MnSiO_4/C done at C/50 rate with $\Delta x = 0.2$. Bragg reflections marked with asterisk denotes in situ cell reflections.

Preliminary electrochemical tests of the Li_2MnSiO_4/C composite prepared by the Pechini method were published elsewhere [13–15]. Additional measurements were performed to evaluate the impact of cut-off voltage and the impact of current density used for the electrochemical characterisation. The impact of higher current density (C/20 instead of C/100) is reflected as about 20 mV higher polarisation, resulting in a lower amount of charge passed during the oxidation process (lithium extraction) (Fig. 5a). However, the difference during the reduction process (lithium insertion) is not as significant as it is during the oxidation process. The amount of charge passed corresponds to approximately 0.7 mol of lithium per a Li_2MnSiO_4 unit. Although we presume that the irreversible loss is, at least partly, increased due to surface reactions, the question is what happens to the active material itself when we cycle it to higher potentials, e.g. to 4.5 V versus lithium reference. The oxidation part of the first cycle shows a much higher amount of consumed charge (calculated as an amount of lithium) if compared to the experiment where the cell was stopped at 4.2 V (Fig. 5a). Again, the reversibility of electrochemical reaction is low. At this moment we cannot give a clear conclusion, if this prolonged first oxidation "plateau" is due to a change in oxidation state from Mn^{II} to Mn^{IV} or due to irreversible reactions occurring at higher potentials. In the consequent cycles (Fig. 5b) the oxidation process of Li_2MnSiO_4 material does not go through a plateau-containing profile (like in

the first oxidation process) which is a clear indication that the sample has undergone some structural rearrangement during the first oxidation process. Formation of an amorphous phase (thermodynamic instability) during the first oxidation of Li_2MnSiO_4/C has been recently observed by preparing several samples in electrochemical cells with known composition and taking ex situ X-ray diffraction patterns on these samples [14,15]. This experimental observation is in agreement with DFT calculations [15], where it was suggested that both lithium atoms were extracted from the crystal cell unit (with a change of oxidation state of manganese from Mn^{II} to Mn^{IV}) simultaneously, before the extraction of lithium from neighbour crystal cell unit started to proceed. The proposed lithium extraction mechanism from Li_2MnSiO_4 – amorphous shell formation – was again checked by taking in situ X-ray diffraction patterns at Li_2MnSiO_4/C composite with a current density corresponding to C/50 in a home-made in situ XRD electrochemical cell. Fig. 6a shows the electrochemical curve and selected patterns that were collected during oxidation/reduction process (each XRD pattern corresponds to a compositional change of $\Delta x = 0.2$). The experiment shows that extraction of lithium leads to a lower intensity of Bragg reflections which almost disappear at a nominal composition of $x \approx 1$ in the $Li_{2-x}MnSiO_4$ structure and this correlates with the proposed lithium extraction mechanism from Li_2MnSiO_4. Quite contrary to Li_2MnSiO_4, however, the structure of Li_2FeSiO_4 remains stable upon cycling (Fig. 6b), which is consistent with observations by Nyten et al. [9] and with predictions of DFT calculations [15]. The lithium extraction/insertion proceeds through a phase transition.

Although Li_2MnSiO_4 shows a structural instability during the first oxidation process, the mere indication that an electrochemical reaction with more than one electron per transition metal is possible, deserves further exploration and optimisation of this material. A better thermodynamic stability can be obtained by stabilisation of the structure by mixing with, for example, Fe. Namely, in such a scenario a combination of two materials, i.e. the electrochemically stable Li_2FeSiO_4 and Li_2MnSiO_4 that enables exchange of oxidation state from Mn^{II} to Mn^{IV}, could lead to an electrochemically stable material with a capacity higher than 200 mAh g^{-1}. Indeed, preliminary experiments in our laboratory have shown that mixing iron with manganese leads to a more stable electrochemical behaviour (Fig. 7a), if compared to the pure Li_2MnSiO_4 sample. Furthermore, cycling of mixed orthosilicate with a composition $Li_2Mn_{0.25}Fe_{0.75}SiO_4$ to a higher cut-off voltage (4.5 instead of 4.2 V) leads to a higher reversible amount of lithium than in the case of pure Li_2MnSiO_4 (also see Fig. 5). The reversibility of the system in the first three cycles is higher than would correspond to $1e^-$ per transition metal ($x = 1.17$ in the first cycle and $x = 1.06$ in the third cycle). It can be concluded that the present results confirm the main message given by Yang's group [20], that is, the ability of orthosilicate to deliver more than one electron per transition metal; however, in their case the stability feature was not proved. It seems, however, that in order to achieve a stable long-term operation, the proper solid solution between Mn and Fe in Li_2MSiO_4 (M = Mn and Fe) should be prepared with carefully selected cut-off voltage (Fig. 7b and c). Structural degradation at higher cut-off voltage was checked by taking in situ X-ray diffraction patterns at $Li_2Mn_{0.25}Fe_{0.75}SiO_4$/C composite with a current density corresponding to C/50 in a home-made in situ XRD electrochemical cell (each scan corresponds to a compositional change of 0.05 mol of lithium). Fig. 8a shows evolution of XRD patterns during the oxidation up to 4.2 V versus metallic lithium and its consequent reduction. The observed phase transition is not as pronounced as in the case of pure Li_2FeSiO_4/C and the structure stability has been proved (Fig. 8b). Further electrochemical tests showed that setting the cut-off voltage to 4.5 V introduced

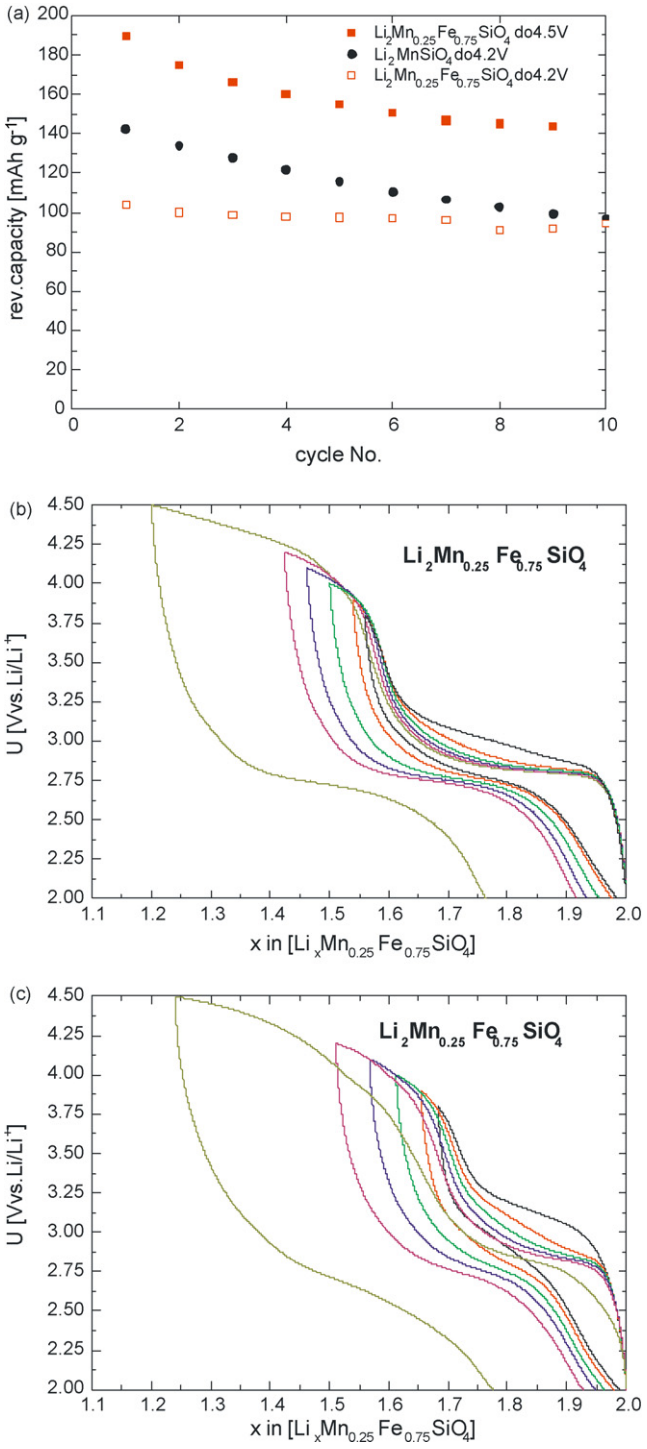

Fig. 7. (a) Reversible capacity of Li_2MnSiO_4/C (filled circles) and a $Li_2Mn_{0.25}Fe_{0.75}SiO_4$/C mixed orthosilicate sample for cut-off voltage 4.2 V (empty squares) and 4.5 V (filled squares) measured at 60 °C with current density corresponding to C/20; discharge–charge curves at different cut-off voltages for (b) $Li_2Mn_{0.25}Fe_{0.75}SiO_4$/C and (c) $Li_2Mn_{0.5}Fe_{0.5}SiO_4$/C.

a capacity fading that is most probably connected with structural degradation. Fig. 8c shows the electrochemical curve and the corresponding collected patterns during the first oxidation/reduction process for $Li_2Fe_{0.75}Mn_{0.25}SiO_4$/C up to 4.5 V versus lithium reference. Comparison of X-ray diffraction patterns before the oxidation process and at the end of the reduction process shows a lower intensity of Bragg reflections at the end of reduction (Fig. 8d). This

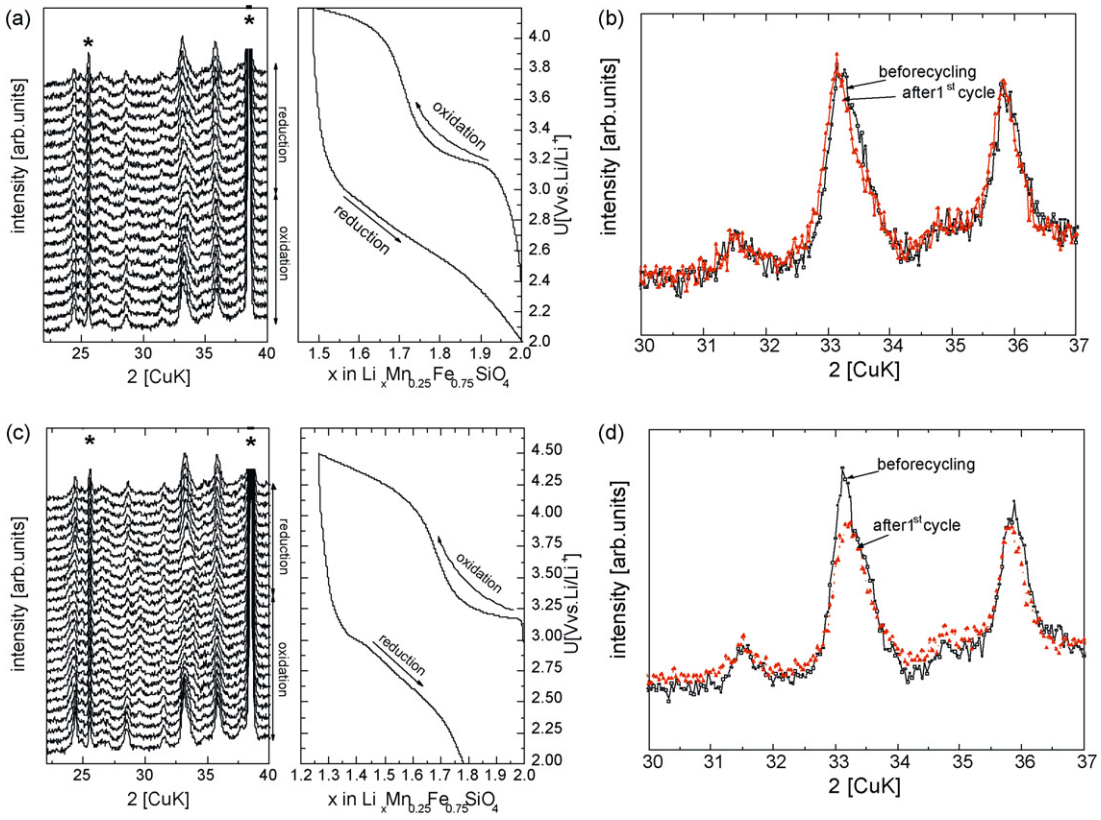

Fig. 8. (a) and (b) In situ X-ray diffraction patterns for $Li_2Mn_{0.25}Fe_{0.75}SiO_4$/C done at C/50 rate with $\Delta x = 0.05$ (cut-off voltage 4.2 V) and comparison of first and last XRD patterns; (c) and (d) in situ X-ray diffraction patterns for $Li_2Mn_{0.25}Fe_{0.75}SiO_4$/C done at C/50 rate with $\Delta x = 0.05$ (cut-off voltage 4.5 V) and comparison of first and last XRD patterns.

result confirms the prediction from electrochemical tests that for Li_2MSiO_4/C solid solutions a higher cut-off voltage is not favourable for long-term operation.

4. Conclusions

Two iso-structural end members of the family of orthosilicates, i.e. Li_2MSiO_4 (M = Mn and Fe) and their solid-solutions have been successfully synthesized and electrochemically characterized. Despite the low specific conductivity, small particles of Li_2FeSiO_4 properly wired with electrons and ions can deliver a capacity close to 100 mAh g^{-1} at moderate current densities at 60 °C. The electrochemical oxidation/reduction process of Li_2FeSiO_4 is accompanied with two-phase transition, while Li_2MnSiO_4 shows a structural instability during the first oxidation process. Combining the structural stability of Li_2FeSiO_4 and the possibility of two electron reaction with Mn, the proper solid solution of $Li_2(Fe/Mn)SiO_4$ with selected cut-off voltage can deliver a reversible capacity of more than 200 mAh g^{-1}, exploring at least partially the change of oxidation state Mn(II) to Mn(IV), however, at present still with a rather poor cycling stability.

Acknowledgements

The author would like to thank M. Gaberscek and J. Jamnik for fruitful discussions and J. Moskon for help in specific conductivity measurements. The financial support from Ministry of Higher Education, Science and Technology of Slovenia (MNT ERA-net project) and the support from the European Network of Excellence 'ALISTORE' network are acknowledged.

References

[1] J.M. Tarascon, M. Armand, Nature 414 (2001) 359–367.
[2] A.K. Padhi, K.S. Nanjundaswamy, J.B. Goodenough, J. Electrochem. Soc. 144 (1997) 1188–1194.
[3] N. Ravet, J.B. Goodenough, S. Besner, M. Simoneau, P. Hovington, M. Armand, Proceedings of the 196th ECS Meeting, Hawaii, October, 1999, pp. 17–22.
[4] C. Delacourt, L. Laffont, R. Bouchet, C. Wurm, J.B. Leriche, M. Morcrette, J.-M. Tarascon, C. Masquelier, J. Electrochem. Soc. 152 (2005) A913–A921.
[5] H. Huang, S.C. Yin, L.F. Nazar, Solid-State Lett. 4 (2001) A170–A172.
[6] C. Delacourt, P. Poizot, M. Morcrette, J.-M. Tarascon, C. Masquelier, Chem. Mater. 16 (2004) 93.
[7] A. Yamada, S.C. Chung, J. Electrochem. Soc. 148 (2001) A960.
[8] A. Nyten, A. Aboumrane, M. Armand, T. Gustafson, J.O. Thomas, Electrochem. Commun. 7 (2005) 156–160.
[9] A. Nyten, S. Kamali, L. Haggstrom, T. Gustafsson, J.O. Thomas, J. Mater. Chem. 16 (2006) 2266–2272.
[10] A. Nyten, M. Stjerndahl, H. Rensmo, H. Siegbahn, M. Armand, T. Gustafsson, K. Edstrom, J.O. Thomas, J. Mater. Chem. 16 (2006) 3483–3488.
[11] K. Zaghib, A. Ait Salah, N. Ravet, A. Mauger, F. Gendron, C.M. Julien, J. Power Sources 160 (2006) 1381–1386.
[12] R. Dominko, D.E. Conte, D. Hanzel, M. Gaberscek, J. Jamnik, J. Power Sources 178 (2008) 842–847.
[13] R. Dominko, M. Bele, M. Gaberscek, A. Meden, M. Remskar, J. Jamnik, Electrochem. Commun. 8 (2006) 217–222.
[14] R. Dominko, M. Bele, A. Kokalj, M. Gaberscek, J. Jamnik, J. Power Sources 174 (2007) 457–461.
[15] A. Kokalj, R. Dominko, M. Gaberscek, M. Bele, G. Mali, M. Remskar, J. Jamnik, Chem. Mater. 19 (2007) 3633–3640.
[16] C. Lyness, B. Delobel, A.R. Armstrong, P.G. Bruce, Chem. Commun. 46 (2007) 4890–4892.
[17] A.R. West, F.P. Glasser, J. Solid State Chem. 4 (1972) 20–28.
[18] Z.L. Gong, Y.X. Li, Y. Yang, Electrochem. Solid-State Lett. 9 (2006) A542–A544.
[19] M.P. Pechini, U.S. Patent No. 3,330,697, July 1967.
[20] J. Moskon, R. Dominko, M. Gaberscek, R.C. Korosec, J. Electrochem. Soc. 153 (2006) A1805–A1811.